Astronomy & Astrophysics manuscript no.
(will be inserted by hand later)

Water vapor in the starburst galaxy NGC253: A new nuclear maser?

C. Henkel[1], A. Tarchi[2,3], K.M. Menten[1], and A.B. Peck[4]

[1] Max-Planck-Institut für Radioastronomie, Auf dem Hügel 69, D–53121 Bonn, Germany
[2] Istituto di Radioastronomia, CNR, Via Gobetti 101, 40129 Bologna, Italy
[3] Osservatorio Astronomico di Cagliari, Loc. Poggio dei Pini, Strada 54, 09012 Capoterra (CA), Italy
[4] SAO/SMA Project, PO Box 824, Hilo, HI 96721, USA

Received date / Accepted date

Abstract. 22 GHz water vapor emission was observed toward the central region of the spiral starburst galaxy NGC 253. Monitoring observations with the 100-m telescope at Effelsberg and measurements with the BnC array of the VLA reveal three distinct velocity components, all of them blueshifted with respect to the systemic velocity. The main component arises from a region close to the dynamical center and is displaced by $<1''$ from the putative nuclear continuum source. The bulk of the maser emission is spread over an area not larger than 70×50 mas^2. Its radial velocity may be explained by masing gas that is part of a nuclear accretion disk or of a counterrotating kinematical subsystem or by gas that is entrained by the nuclear superwind or by an expanding supernova shell. A weaker feature, located $\sim5''$ to the northeast, is likely related to an optically obscured site of massive star formation. Another maser component, situated within the innermost few $10''$ of the galaxy, is also identified.

Key words. Galaxies: active – Galaxies: individual: NGC 253 – Galaxies: ISM – Galaxies: Starburst – Radio lines: galaxies

1. Introduction

Extragalactic H_2O masers, observed in the $6_{16}\rightarrow5_{23}$ transition at 22.23508 GHz ($\lambda\sim1.3$ cm), are best known as a means to probe accretion disks in Seyfert galaxies (e.g. Miyoshi et al. 1995; Herrnstein et al. 1999). More than 30 luminous 'megamasers' with (isotropic) luminosities $L_{\rm H_2O} > 10\,{\rm L}_\odot$ are known to date (e.g. Braatz et al. 1996; Greenhill et al. 2003). All of those studied with high angular resolution are located within a few parsecs of the nucleus of their parent galaxy, tracing either a circumnuclear accretion disk or hinting at an interaction between the nuclear radio jet(s) and an encroaching molecular cloud (for the latter, see Peck et al. 2003).

Not all of the known extragalactic water vapor masers show extremely high luminosities. Weaker masers, the 'kilomasers', were detected in M 33, M 82, IC 10, NGC 253, M 51, IC 342, NGC 2146, and NGC 6300 (Churchwell et al. 1977; Huchtmeier et al. 1978; Claussen et al. 1984; Henkel et al. 1986; Ho et al. 1987; Becker et al. 1993; Tarchi et al. 2002a,b; Greenhill et al. 2003) with (isotropic) luminosities up to $L_{\rm H_2O} \sim 10\,{\rm L}_\odot$.

Extragalactic H_2O masers provide important information about their parent galaxies. Studies of 'disk-masers' yield mass estimates of the nuclear engine and, for NGC 4258, a calibration of the cosmic distance scale. 'Jet-masers' provide insights into the interaction of nuclear jets with dense warm molecular material and help to determine the speed of the material in the jets. Masers in the large scale galactic disks mark locations of ongoing massive star formation and can be used to determine, through measurements of proper motion, distances to (Greenhill et al. 1993) and three dimensional velocity vectors of (Brunthaler et al. 2003) these galaxies.

Most kilomasers, i.e. those in IC 10, M 33, IC 342, NGC 2146 and M 82, are known to be associated with star forming regions (e.g. Argon et al. 1994; Baudry & Brouillet 1996; Tarchi et al. 2002a,b). In M 51, however, the maser components arise within $0\farcs25$ from the nucleus, possibly being related to the receding jet or to an accretion disk (Hagiwara et al. 2001). Although it was detected a long time ago (Ho et al. 1987), the H_2O maser emission in the prototypical starburst galaxy NGC 253 had not yet been studied with high angular resolution. Here we report the first Very Large Array (VLA[1]) observations of

Send offprint requests to: C. Henkel, e-mail: chenkel@mpifr-bonn.mpg.de

[1] The National Radio Astronomy Observatory (NRAO) is operated by Associated Universities, Inc., under a cooperative agreement with the National Science Foundation.

the maser(s) in NGC 253, complemented by monitoring measurements with the 100-m telescope at Effelsberg[2].

2. Observations

2.1. VLA observations and image processing

NGC 253 was observed with the VLA in its hybrid CnB configuration on 2002, September 22. A frequency setup with a bandwidth of 12.5 MHz was employed; the resulting channel spacing is 2.63 km s^{-1}. With 63 channels, a total range of 166 km s^{-1} was covered, centered at an LSR velocity of 120 km s^{-1}. Typically, 3 minute observations of NGC 253 were alternated with observations of the phase calibrator 01205–27014. Absolute amplitude calibration was obtained using 3C48. The phase center for the NGC 253 observations was $(\alpha,\delta)_{2000} = 00^{\rm h}\ 47^{\rm m}\ 33\overset{\rm s}{.}1805$, $-25^\circ\ 17'\ 15\overset{''}{.}991$. The so-called 'channel 0' data, comprising 75% of the passband, were used to produce a map of the continuum plus H_2O maser emission. Several iterations of self calibration resulted in a high quality map. The final phase and amplitude corrections were applied to conventionally calibrated data. The average of the line-free channels was then subtracted in the *uv*-plane, resulting in a line-only database, from which images of the line emission were made. A continuum image was made from the line-free channels. All data reduction was performed using NRAO's Astronomical Image Processing system (AIPS). The restoring beam size was $1\overset{''}{.}1 \times 0\overset{''}{.}8$ with a position angle East of North of 88°.

2.2. Effelsberg observations

Observations with the 100-m telescope at Effelsberg were obtained between January 1994 and September 2002. The beam size was 40″. Until 1997, observations were carried out in a position switching mode with a K-band maser receiver. Later, data were taken with a K-band HEMT receiver in a dual beam switching mode with a beam throw of 2′ and a switching frequency of ∼1 Hz. Due to low elevations (∼12°), the system temperature, including atmospheric contributions, was 50–180 K on an antenna temperature scale ($T_{\rm A}^*$; beam efficiency: $\eta_{\rm b}$∼0.3). Flux calibration was obtained measuring W3(OH) (3.2 Jy; Mauersberger et al. 1988). Although gain variations of the telescope as a function of elevation were taken into account (Eq. 1 of Gallimore et al. 2001), calibration at low elevations may be uncertain by ±30%. Pointing on nearby continuum sources was found to be better than 10″.

3. Results

Fig. 1 shows the 22.2 GHz continuum map which, accounting for the different angular resolutions, is consistent with the map of Ulvestad & Antonucci (1997, hereafter UA97)

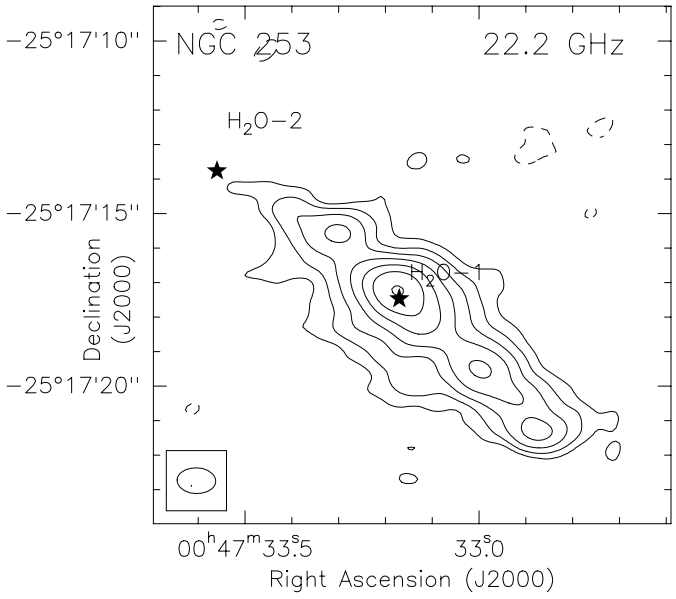

Fig. 1. Map of the 22.2 GHz continuum emission (epoch: Sept. 22, 2002). Contour values are –2, –1, 1, 2, 4...32 times the 3σ noise level of 0.9 mJy beam^{-1}. The positions of the water masers H_2O–1 and H_2O–2 are indicated. Size and orientation of the restoring beam are shown in the lower left corner.

at the same frequency. We used the AIPS task SAD to search all of the continuum-subtracted channel maps for emission above 18 mJy beam^{-1}, which is 4 times the 1σ rms noise level. H_2O emission originates from two locations (see Figs. 1 and 2): H_2O–1 ($V_{\rm LSR} \sim 120$ km s^{-1}) is at $(\alpha,\delta)_{2000} =$

$$00^{\rm h}47^{\rm m}33\overset{\rm s}{.}1701 \pm 0\overset{\rm s}{.}0004, -25^\circ 17'\ 17\overset{''}{.}465 \pm 0\overset{''}{.}004$$

or $(\alpha,\delta)_{1950} =$

$$00^{\rm h}45^{\rm m}05\overset{\rm s}{.}7897 \pm 0\overset{\rm s}{.}0004, -25^\circ 33'\ 39\overset{''}{.}474 \pm 0\overset{''}{.}004$$

and has an integrated H_2O luminosity of 5.62 Jy km s^{-1} ($L_{\rm H_2O} \sim 0.8\,L_\odot$). H_2O–2 ($V_{\rm LSR} \sim 170$ km s^{-1}) is at $(\alpha,\delta)_{2000} =$

$$00^{\rm h}47^{\rm m}33\overset{\rm s}{.}559 \pm 0\overset{\rm s}{.}004, -25^\circ 17'\ 13\overset{''}{.}76 \pm 0\overset{''}{.}03$$

and has an integrated H_2O luminosity of 145 mJy km s^{-1} ($L_{\rm H_2O}$∼0.02 $L_\odot$). The emission from H_2O–2 is detected at a 6–8σ level depending on whether the absorption feature next to the line (upper panel of Fig. 2) is included or flagged (bad channel) when determining the noise level. The position errors given above are formal values determined using the AIPS task JMFIT on a map of integrated emission, in the case of H_2O–1 from 88 km s^{-1} to 149 km s^{-1} and for H_2O–2 from 167 km s^{-1} to 174 km s^{-1}. We estimate the *absolute* position uncertainty to be ∼0″.5.

Fig. 3 presents a close-up of the region around NGC 253 H_2O–1, demonstrating that the bulk of the emission is spread over an area not larger than 70×50 milliarcseconds (mas), corresponding to 0.8×0.6 pc (D=2.5 Mpc). Shown

[2] The 100-m telescope at Effelsberg is operated by the Max-Planck-Institut für Radioastronomie (MPIfR) on behalf of the Max-Planck-Gesellschaft

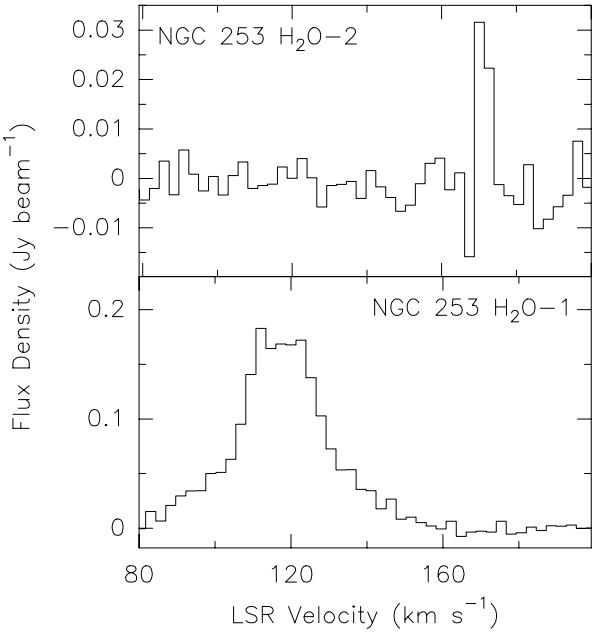

Fig. 2. Lower panel: VLA spectrum, taken on Sept. 22, 2002, of the centrally located water maser associated with NGC 253 H_2O–1. Upper panel: VLA spectrum of the north-eastern water maser associated with NGC 253 H_2O–2. The velocity scale is LSR (Local Standard of Rest). $V_{\rm HEL} = V_{\rm LSR} + 7.1\,{\rm km\,s^{-1}}$. For both spectra, the channel spacing is $2.63\,{\rm km\,s^{-1}}$.

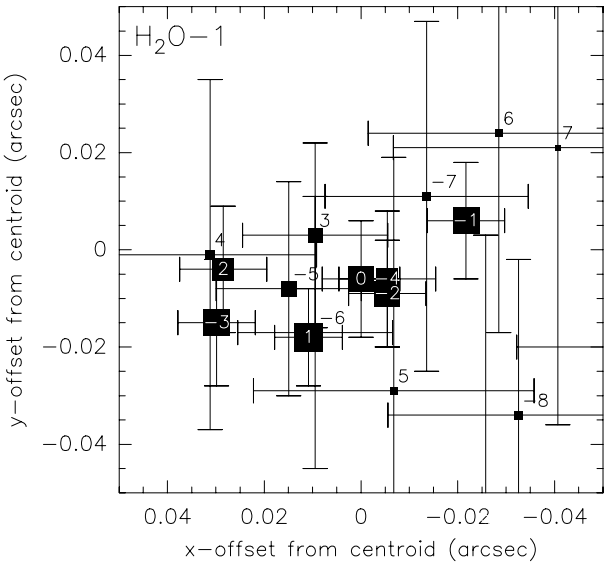

Fig. 3. Close-up of the region around NGC 253-H_2O–1. Shown as squares are the maser positions from JMFIT with error bars. Position offsets in $(\alpha_{2000}, \delta_{2000})$ are relative to the centroid position given in Sect. 3. The numbers give velocity offsets in units of $2.63\,{\rm km\ s^{-1}}$ from $117.37\,{\rm km\ s^{-1}}$, i.e. position 1 corresponds to $120\,{\rm km\,s^{-1}}$. The side lengths of the symbols are proportional to the emission in that channel ($187\,{\rm mJy\ beam^{-1}}$ for position 1).

as squares are relative maser positions from JMFIT with error bars.[3] The numbers give channel offsets (in units of $2.63\,{\rm km\ s^{-1}}$). Position 1 corresponds to 120 km s^{-1}. The fitted flux density in all channels is >5 times the rms noise of $4.4\,{\rm mJy\ beam^{-1}}$. Low level ($<5\sigma$) emission with offsets $<0\farcs2$ is also observed but here the positions have such error bars that the larger offsets from the reference position may not be significant.

Fig. 4 shows the Effelsberg spectra covering a time interval of more than eight years. Emission from H_2O–1, sometimes split into two velocity components, dominates all spectra, at a level of $\sim$100 mJy. This is consistent with data collected before (Ho et al. 1987; Nakai & Kasuga 1988). The agreement between the VLA spectrum (Fig. 2) and that observed with Effelsberg five days later (Fig. 4, upper panel) is reasonably good. While the VLA spectrum is more sensitive, the Effelsberg spectrum covers a wider velocity range. The Effelsberg spectrum contains a weak tentative feature at $170\,{\rm km\,s^{-1}}$ that is convincingly detected by the VLA (H_2O–2). Differences between the spectra are, however, also apparent: In the VLA spectrum the flux density of H_2O–1 is twice that in the Effelsberg spectrum, while the tentative $85\,{\rm km\,s^{-1}}$ component, apparent in Fig. 4, is not confirmed. The Effelsberg spectrum also shows a $225\,{\rm km\,s^{-1}}$ feature (H_2O–3) that is close to the systemic velocity of the galaxy ($V_{\rm sys} \sim$ 225–$245\,{\rm km\,s^{-1}}$; e.g. Canzian et al. 1988; Anantharamaiah & Goss 1996; Prada et al. 1996). Since this feature was not known prior to the interferometric mesurements, its velocity range is not part of the VLA observations.

4. Discussion

The Sculptor galaxy NGC 253 is a highly inclined ($i\sim$78°) nearby ($D\sim$2.5 Mpc) barred Sc spiral and is one of the brightest sources of far infrared emission beyond the Magellanic Clouds (e.g. Pence 1981; Scoville et al. 1985; IRAS 1989; Mauersberger et al. 1996; Das et al. 2001). Its spectral energy distribution has been studied from radio waves (e.g. UA97) to TeV γ-rays (Itoh 2002). At many wavelengths the nuclear environment is dominated by a starburst that is confined to a $\sim$100 pc region located in the plane of the galaxy and that is centered slightly southwest of the dynamical center (e.g. Keto et al. 1993, 1999; Telesco et al. 1993; Böker et al. 1998). Radio continuum measurements indicate that NGC 253 contains a large number of potential supernova remnants and HII regions near its center. The strongest of these radio sources, located right at the dynamical center, remains unresolved

[3] While formal errors returned from some software packages have to be viewed with caution, we are convinced that JMFIT returns meaningful errors, derived using the rms noise around the fitted position. The position error in a coordinate from Gaussian fitting is theoretically $\sim 0.5\theta_{\rm B}/SNR$, where $\theta_{\rm B}$ is the beam size and SNR is the map's signal-to-noise ratio (Reid et al. 1980). Using this formula, we 'manually' calculated fitting errors for a few components and found good agreement with the values returned by JMFIT.

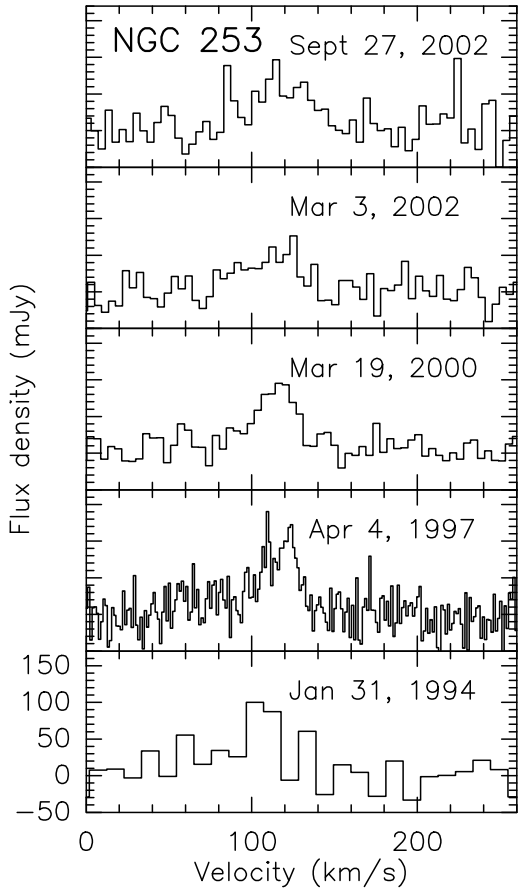

Fig. 4. H_2O spectra with LSR velocity scale taken between 1994 and 2002. No redshifted emission was seen beyond 260 km s^{-1} out to 400 km s^{-1} (Jan. 1994, Apr. 1997), to 950 km s^{-1} (Mar. 2000), to 800 km s^{-1} (Mar. 2002) and to 400 km s^{-1} (Sept. 2002). Channel spacings and 1σ noise levels are (upper to lower panel) 4.2, 4.2, 4.2, 1.3, and 10.5 km s^{-1} and 21.7, 19.2, 11.6, 22.2 and 20.6 mJy, respectively. The systemic velocity is $V_{\rm sys} \sim 240$ km s^{-1} (see Sect. 3).

in VLA images, shows a relatively flat radio spectral index and has a brightness temperature in excess of 10^4 K (Turner & Ho 1985; Antonucci & Ulvestad 1988; Ulvestad & Antonucci 1991, 1994; UA97). The source is likely to indicate the position of the active galactic nucleus (AGN) in NGC 253.

4.1. H_2O–1

The position of H_2O–1 can be compared with the positions of nine radio continuum sources that were detected in the VLA A configuration by UA97 at λ=1.3 cm. Three of the sources are close to the maser, TH2, TH3 and TH4. TH2 is nominally offset from H_2O–1 by $(\Delta\alpha, \Delta\delta)$ = $(+0\farcs06, +0\farcs38)$, TH3 by $(+0\farcs00, -0\farcs29)$ and TH4 by $(-0\farcs10, +0\farcs04)$. TH2 is the strongest of the 64 radio sources compiled by UA97. It is the source that is associated with the putative AGN. TH4 may be a supernova remnant, while the spectrum of TH3 is not well determined.

Our absolute position uncertainty is $0\farcs5$ (Sect. 3). The registration of our maps with those of UA97 obtained with different phase calibrators and the conversion of B1950.0 to J2000.0 coordinates (using NED[4]) may further increase the total error budget, but only slightly. Comparing the coordinates given by Turner & Ho (1985) and UA97 for the hypothesized nuclear continuum source, we find a difference of $0\farcs15$, while the coordinate conversion should introduce an error of order $0\farcs05$ (e.g. Fricke 1982; Ma et al. 1998).

H_2O–1 appears to be closest to TH4, but TH2 and TH3 are also located within the region defined by our absolute position uncertainty. H_2O–1 is then not necessarily associated with TH4. An association with TH2 or TH3 is also possible. We thus conclude that *the maser arises from the nuclear region of the galaxy. A direct association with the nucleus is not ruled out by our measurements.*

Having identified a maser component close to the hypothesized galactic nucleus, its lineshape, radial velocity and association with other sources deserve to be briefly discussed. H_2O–1 shows a smooth broad profile that is rarely seen in galactic or extragalactic H_2O maser sources. The profile resembles those seen toward the jets of AGN (i.e. NGC 1052 and Mrk 348; Braatz et al. 1996; Peck et al. 2003) and toward prominent star forming regions in M 33 and NGC 2146 (Huchtmeier et al. 1978; Tarchi et al. 2002b). The profile does *not* resemble any lineshape observed toward circumnuclear disks (e.g. NGC 4258, Mrk 1419 and NGC 1068; Miyoshi et al. 1995; Gallimore et al. 2001; Henkel et al. 2002). In view of the small number of sources studied thus far, however, the strength of this argument is difficult to assess.

H_2O–1 appears to be located slightly southwest of the nucleus, i.e. on that side of the edge-on galaxy that is redshifted (e.g. Fig. 1 of Das et al. 2001). If we adopt this view, the blueshift of $\sim$120 km s^{-1} w.r.t. $V_{\rm sys}$ appears to be highly peculiar. The enormous discrepancy between observed and expected velocity that is of order 200–300 km s^{-1} can then be explained by the following possibilities: (1) The maser is part of a circumnuclear acretion disk, likely centered at TH2; (2) the emission originates from a counter-rotating nuclear core component; (3) the masing gas is entrained by an expanding supernova shell or (4) the masing gas is entrained by the nuclear wind.

If the maser is tracing an accretion disk around a supermassive central object as in NGC 4258, we may exclusively view the blueshifted side of this disk that may be displaced by a few milliarcseconds from the dynamical center. Such a position is well within the limits of our observational accuracy. The presence of a prominent

[4] This research has made use of the NASA/IPAC Extragalactic Database (NED) which is operated by the Jet Propulsion Laboratory, California Institute of Technology, under contract with the National Aeronautics and Space Administration.

source of hard X-rays at the very center and nuclear column densities of several $10^{23}\,\mathrm{cm}^{-2}$ (Weaver et al. 2002) are consistent with such a scenario.

From observations of the 8.3 GHz H 92α radio recombination line with a resolution of $1\farcs8\times1\farcs0$, Anantharamaiah & Goss (1996) identify three kinematic subsystems near the center of NGC 253, one with solid body rotation in the same sense as the galactic large scale disk, a second exhibiting rotation in a plane perpendicular to this disk and a third one in the innermost $2''$ that may actually counterrotate. H_2O–1 is located within this innermost region.

An association with the envelope of a rapidly expanding supernova remnant (e.g. TH4) interacting with a dense molecular cloud might explain the peculiar velocity of H_2O–1. Such sources are, however, not common in the Galaxy, likely because gas densities are too low (Claussen et al. 1999). M 82, a nearby starburst galaxy like NGC 253, also contains a large number of supernova remnants (e.g. Kronberg et al. 1985). The H_2O masers appear, however, to be associated with prominent star forming regions (Baudry & Brouillet 1996). While the parent molecular clouds are often located at the periphery of supernova remnants, a direct association with their expanding shells is not obvious. While conditions near the nucleus of NGC 253 may differ from those in the Milky Way and M 82, a scenario involving expanding supernova shells is therefore not likely.

A nuclear plume is seen in the far infrared and X-ray continuum (e.g. Rice 1993; Pietsch et al. 2000), in optical emission lines (e.g. Heckman et al. 1990; Schulz & Wegner 1992), and in the λ18 cm lines of OH (Turner 1985). Most of the gas in the OH plume, that is most prominent north of the nucleus, is receding with respect to $V_{\rm sys}$ and is likely arising from the far side of the galaxy disk. Therefore the base of this OH plume should not be blueshifted w.r.t. $V_{\rm sys}$, which would be necessary in order to be compatible with the blueshifted H_2O component observed towards H_2O–1. A direct association between H_2O–1 and the OH plume is thus unlikely.

Radio jets can be a strong agent to drive maser action when hitting high density clumps or entraining molecular gas (e.g. Elitzur 1995; Peck et al. 2003). Less violent, optically detectable ionized outflowing material might, however, also trigger maser emission (Schulz & Henkel 2003). In NGC 253, optical emission lines and the X-ray continuum indicate the presence of a cone-like structure that is viewed almost edge-on and that originates from the nuclear region (Pietsch et al. 2000 and references therein). Likely representing a superwind triggered by the starburst, the cone surface may indicate the boundary between the outflowing gas and the ambient medium. The cone is seen southeast of the nuclear region, i.e. on the opposite side of the OH plume, and shows blueshifted emission. This cone is, however, observed at distances of several arcseconds SE of the nucleus and its presence and nature in the very nuclear region remains an enigma. We conclude that it is not obvious how an interaction of this wind with a molecular cloud could explain the line emission from H_2O–1.

From analogy to the Galaxy, an association of H_2O–1 with a red giant star can be excluded on the basis of the high luminosity of the maser. A star forming region with a broad dominant maser component that does not strongly vary with time and that shows no narrow occasionally flaring spikes is also not known in the Galaxy.

To summarize the discussion on H_2O–1, we find that an association with the nuclear source is an attractive scenario, while a connection with a counterrotating kinematical subcomponent, an expanding supernova remnant or the superwind cannot be ruled out. Among possible counterparts to H_2O–1, we should also consider compact regions of molecular line emission. At first sight, an association between the 18 cm OH satellite lines masers (region 7 according to Frayer et al. 1998) and H_2O–1 may appear farfetched since the main OH component has a radial velocity of $V\sim210\,\mathrm{km\,s^{-1}}$. Weaker OH emission is, however, seen between 100 and $200\,\mathrm{km\,s^{-1}}$ so that an association *might* be possible.

4.2. H_2O–2

H_2O–2 is situated northeast of the nucleus. Here the radial velocity is consistent with its position (see e.g. Paglione et al. 1995). An association with young massive stars is likely. The maser may arise from an optically highly obscured region. No X-ray, optical, near infrared or radio counterpart is apparent (e.g. Kalas & Wynn-Williams 1994; UA97; Dudley & Wynn-Williams 1999; Vogler & Pietsch 1999). The maser may be located in a region of intense SiO emission (see the SiO $171.25\,\mathrm{km\,s^{-1}}$ panel in Fig. 3 of García-Burillo et al. 2000). SiO is a tracer of shock chemistry that can also enhance H_2O abundances by several orders of magnitude.

5. Concluding remarks

Obviously, A configuration VLA data are needed to determine more accurate relative positions between the dominant 22 GHz H_2O maser (H_2O–1) and the dominant radio continuum source of the galaxy. This would allow us to confirm or to reject a direct association between H_2O–1 and the putative AGN. Such measurements should also include an attempt to spatially resolve the emission from H_2O–1 and a determination of the position of the near systemic feature detected in the most recent Effelsberg spectrum. In any case, the small projected distance between H_2O–1 and the central radio source shows that the maser is arising from the nuclear region of NGC 253. As early as 1987, Ho et al. postulated the existence of a numerous family of weak nuclear masers. This family was supposed to form the low luminosity tail of a megamaser distribution that is likely characterized by highly non-isotropic emission. Such masers are difficult to detect because they are too weak to be observed at distances much in excess of 10 Mpc. It is possible that after identifying weak nuclear

maser emission in M 51 (Hagiwara et al. 2001), we have found a second such case. Being located at a distance of only $D{\sim}2.5$ Mpc, follow-up studies with high spatial resolution will be possible.

Acknowledgements. We wish to thank an anonymous referee and J.S. Ulvestad for critical comments and are grateful to the VLA and 100-m Effelsberg staff for their cheerful assistance.

References

Anantharamaiah, K. R., & Goss, W. M. 1996, ApJ, 466, L13
Antonucci, R. R. J., & Ulvestad, J. S. 1988, ApJ, 330, L97
Argon, A. L., Greenhill, L. J., Moran, J. M., et al. 1994, ApJ, 422, 586
Baudry, A., & Brouillet, N. 1996, A&A, 316, 188
Becker, R., Henkel, C., Wilson, T. L., & Wouterloot, J. G. A. 1993, A&A, 268, 483
Böker, T., Krabbe, A., & Storey, J.W.V. 1998, ApJ, 498, L115
Braatz, J. A., Wilson, A. S., & Henkel, C. 1996, ApJS 106, 51
Brunthaler, A., Falcke, H., Reid, M., Greenhill, L. J., & Henkel, C. 2003, Proc. 6th European VLBI Network Symposium, eds. E. Ros et al., in press
Canzian, B., Mundy, L. G., & Scoville, N. Z. 1988, ApJ, 333, 157
Churchwell, E., Witzel, A., Huchtmeier, W., et al. 1977, A&A, 54, 969
Claussen, M. J., Heiligman, G. M., & Lo, K. Y. 1984, Nature, 310, 298
Claussen, M. J., Goss, W. M., Frail, D. A., & Seta, M. 1999, AJ, 117, 1387
Das, M., Anantharamaiah, K. R., & Yun, M. S. 2001, ApJ, 549, 896
Dudley, C. C., & Wynn-Williams, C. G. 1999, MNRAS, 304, 549
Elitzur, M. 1995, Rev. Mex. Astron. Astrofis., 1, 85
Frayer, D. T., Seaquist, E. R., & Frail, D. A. 1998, AJ 115, 559
Fricke, W. 1982, A&A, 107, L13
Gallimore, J. F., Henkel, C., Baum, S. A., et al. 2001, ApJ, 556, 694
García-Burillo, S., Martin-Pintado, J., Fuente, A., & Neri, R. 2000, A&A, 355, 499
Greenhill, L. J., Moran, J. M., Reid, M. J., Menten, K. M., & Hirabayashi, H. 1993, ApJ, 406, 482
Greenhill, L. J., Kondratko, P. T., Lovell, J. E. J., et al. 2003, ApJ, 582, L11
Hagiwara, Y., Henkel, C., Menten, K. M., & Nakai, N. 2001, ApJ 560, L37
Heckman, T. M., Armus, L., & Miley, G. K. 1990, ApJS 74, 833
Henkel, C., Wouterloot, J. G. A., & Bally, J. 1986, A&A, 155, 193
Henkel, C., Braatz, J. A., Greenhill, L. J., & Wilson, A. S. 2002, A&A, 394, L23
Herrnstein, J. R., Moran, J. M., Greenhill, L. J., et al. 1999, Nature, 400, 539
Ho, P.T.P., Martin, R. N., Henkel, C., & Turner, J. L. 1987, ApJ, 320, 663
Huchtmeier, W. K., Witzel, A., Kühr, H., Pauliny-Toth, I. I., & Roland, J. 1978, A&A, 64, L21
IRAS 1989, Catalogued Galaxies and Quasars Observed in the IRAS Survey, Version 2, L. Fullmer & C. Lonsdale, JPL D–1932
Itoh, C., Enomoto, R., Yanagita, S., et al. 2002, A&A, 396, L1
Kalas, P., & Wynn-Williams, C. G. 1994, ApJ 434, 546
Keto, E., Ball, R., Arens, J., et al. 1993, ApJ, 413, L23
Keto, E., Hora, J. L., Fazio, G. G., Hoffmann, W., & Deutsch, L. 1999, ApJ, 518,183
Kronberg, P. P., Biermann, P., & Schwab, F. R. 1985, ApJ, 291, 693
Ma, C., Arias, E. F., Eubanks, T. M., et al. 1998, AJ, 116, 516
Mauersberger, R. Wilson, T.L., & Henkel, C. 1988, A&A, 201, 123
Mauersberger, R., Henkel, C., Wielebinski, R., Wiklind, T., & Reuter, H.-P. 1996, A&A 305, 421
Miyoshi, M., Moran, J. M., Herrnstein, J. R., et al. 1995, Nature, 373, 127
Nakai, N., & Kasuga, T. 1988, PASJ, 40, 139
Paglione, T. A. D., Tosaki, T., & Jackson, J. M. 1995, ApJ, 454, L117
Peck, A. B., Henkel, C., Ulvestad, J. S., et al. 2003, ApJ, 590, 149
Pence, W. D. 1981, ApJ, 247, 473
Pietsch, W., Vogler, A., Klein, U., & Zinnecker, H. 2000, A&A, 360, 24
Prada, F., Manchado, A., Canzian, B., et al. 1996, ApJ, 458, 537
Reid, M. J., Haschick, A. D., Burke, B. F., et al. 1980, ApJ, 239, 89
Rice, W. 1993, AJ, 105, 67
Schulz, H., & Henkel, C. 2003, A&A, 400, 41
Schulz, H., & Wegner, G. 1992, A&A, 266, 167
Scoville, N. Z., Soifer, B. T., Neugebauer, G., et al. 1985, ApJ 289, 129
Tarchi, A., Henkel, C., Peck, A. B., & Menten, K. M. 2002a, A&A, 385, 1049
Tarchi, A., Henkel, C., Peck, A. B., & Menten, K. M. 2002b, A&A, 389, L39
Telesco, C. M., Dressel, L. L., & Wolstencroft, R. D. 1993, ApJ, 414, 120
Turner, B. E. 1985, ApJ, 299, 312
Turner, J. L., & Ho, P. T. P. 1985, ApJ, 299, L77
Ulvestad, J. S., & Antonucci, R. R. J. 1991, AJ, 102, 875
Ulvestad, J. S., & Antonucci, R. R. J. 1994, ApJ, 424, L29
Ulvestad, J. S., & Antonucci, R. R. J. 1997, ApJ, 488, 621 (UA97)
Vogler, A., & Pietsch, W. 1999, A&A, 342, 101
Weaver, K. A., Heckman, T. M., Strickland, D. K., & Dahlem, M. 2002, ApJ, 576, L19